19

Shape and Volume of Living Aldosterone-Sensitive Cells Imaged with the Atomic Force Microscope

Stefan W. Schneider, Rainer Matzke, Manfred Radmacher, and Hans Oberleithner

1. Introduction

The steroid hormone aldosterone, which is synthesized in the suprarenal glands and secreted in response to a reduction in circulating blood volume, increases water and sodium reabsorption in the kidney ***(1,2)***. Although kidney is the major target organ, various other cell types, including different epithelia, smooth muscle, and endothelium, respond to the hormone ***(3–6)***. The acute aldosterone-induced responses of target cells are an intracellular calcium change and an intracellular pH increase ***(3,7,8)*** along with activation of plasma membrane Na^+/H^+ exchange and plasma membrane proton conductance ***(9,10)***. Therefore, it is not surprising that researchers have postulated that these acute transmembrane shifts of electrolytes are accompanied by cell swelling ***(2,11)***. Cell swelling or shrinkage plays a critical role in endothelial cell (EC) function. ECs tightly coat the luminal surface of blood vessels, playing an important role in the regulation of vascular tone, in vascular remodeling, in the pathogenesis of arteriosclerosis, and in arterial hypertension of humans ***(12)***. It has been shown that swelling of EC may disturb cell-to-cell interactions, resulting in an increase of transendothelial permeability, a precursor mechanism in the development of arteriosclerosis ***(13,14)***. Moreover, environmental stress (e.g., mechanical forces or hyperosmolarity) induces changes in cell volume and stimulates tissue plasminogen activator synthesis ***(15–18)***. Direct evidence for the importance of cell-volume regulation of endothelial cells is the existence of a volume-sensitive protein kinase ***(19)***.

There are different methods to measure cell volume. A simple technique is to measure cell volume by Coulter counter, which is commonly used for blood cells in suspension. In contrast with spherical cells in suspension, ECs under

From: *Methods in Molecular Biology, vol. 242: Atomic Force Microscopy: Biomedical Methods and Applications*
Edited by: P. C. Braga and D. Ricci © Humana Press Inc., Totowa, NJ

physiological conditions adhere to a substrate and develop a complex morphology (i.e., they polarize, form tight junctions and gap junctions, and develop monolayers). Thus, more sophisticated techniques must be applied. One is optical sectioning using quantitative differential interference contrast light microscopy ***(20,21)***. Here, we present an alternative new method using atomic force microscopy (AFM) for measuring cell volume in individual ECs with femto-liter resolution ***(22–25)***. AFM enables measurement of cell volume and cell-volume fluctuations in living adherent cells irrespective of the cell shape changes that occur during time-lapse measurements ***(26)***. Because surface topography and cell volume are simultaneously recorded, localized volume changes become visible within a single cell.

This chapter describes the protocol for the measurement of cell volume of living, adherent endothelial cells upon aldosterone stimulation. We used the BioScope® (DI, St. Barbara, CA.) in combination with an inverted microscope (Axiovert 100, Zeiss, Jena Germany) in two different scanning modes (contact and force volume modes) and with commercially available scanning tips (Microlever, Park Scientific, Sunnyvale, CA).

2. Materials

2.1. Chemicals

1. Aldosterone (Sigma, Taufkirchen, Germany) soluble in ethanol (stock solution = 10 μ*M*, stored at 4°C for 2 wk). Experimental concentration 10–0.1 n*M* (ethanol concentration less than 0.1%).
2. HEPES-buffered solution (140 m*M* NaCl, 5 m*M* KCl, 1 m*M* $MgCl_2$, 1 m*M* $CaCl_2$, 5 m*M* glucose, 10 m*M* HEPES (*N*-2-hydroxyethylpiperazine-*N*'-2-ethanesulfonic acid); pH, 7.4 further referred to as HEPES-buffered Ringer solution (HBRS).
3. Medium for endothelial cells (M199, Gibco, Karlsruhe, Germany).

2.2. AFM

1. BioScope (Digital Instruments, St. Barbara, CA), including software for volume analysis and force volume measurements.
2. Cantilever (Microlever, spring constant = 0.01 N/m, Park Scientific, Sunnyvale, CA).
3. Perfusion and heating chamber (homemade for continuous cell superfusion at 37°C); "Heparin perfusor" (Perfusor E; B. Braun, Melsungen, Germany) to control the flow rate (approx 1–5 mL/h). Consider that the superfusion as well as the heating chamber may cause electrical and mechanical noise.
4. The BioScope is placed on a homemade antivibration table. The whole setup is placed in a homemade box (Faraday cage), which is insulated (with foamed matter) against outside noise.
5. Heating lamp, fixed inside the box, to increase the ambient temperature to about 30°C (this avoids large thermal fluctuations in the bath solution which is maintained at 37°C).

2.3. Endothelial Cells

1. We use freshly prepared bovine (aorta) or human endothelial cells from the umbilical vein (HUVECs). For preparation protocol, please *see* **ref. *27***.
2. The culture medium (M199, Gibco, Karlsruhe, Germany) contains 10% heat-inactivated fetal calf serum (Boehringer Mannheim, Mannheim, Germany), antibiotics (penicillin 100 U/mL, streptomycin 100 µg/mL), 5 U/mL heparin (Biochrom, Berlin, Germany), and 1 mL/100 mL growth supplement derived from bovine retina as described ***(28)***.
3. Cells are cultivated first in T25 Petri dishes coated with 0.5% gelatin (passage p0). After reaching confluency cells are split using trypsin and then cultivated (passage p1) on glass cover slips (coated with 0.5% gelatin and fixed with 2% glutaraldehyde). Only living cells of passage p1 are used for experiments.
4. For AFM experiments the glass cover slip with cells is mounted in the perfusion chamber and superfused with 37°C HBRS.
5. Important: always keep cells in solution!

3. Methods

3.1. AFM Handling

Follow the AFM manual to get started. All experiments (on glass and on cells) are performed in contact mode.

3.2. Calibration of the Cantilever on a Glass Cover Slip

1. Start to scan a clean glass cover slip in fluid. This will help you to evaluate your cantilever and AFM setup. Moreover, you have to calibrate your force curve on glass before imaging cells.
2. For a high-quality image (i.e., integral and proportional gains as high as possible) you should use cover slips that are at least 0.8 mm thick. Important: Thin glass cover slips may oscillate and cause mechanical noise. When glass oscillations occur, gain values above one are not advisable (a further increase in gain values will cause piezo oscillations).
3. Before you mount the cantilever in the holder, dip the cantilever in a 37°C buffer solution. The procedure avoids air bubbles at your cantilever.
4. Mount the BioScope head with the cantilever holder on your inverted microscope. The cantilever should be close to the glass surface and submerged in a 37°C buffer solution.
5. Never let fluid get into the piezo!
6. Focus the laser on the cantilever to get a sharp laser spot in the photo diode. You should get a sum signal of at least 2 V. Bring the laser spot on the display to the center (see manual for details).
7. Before imaging glass or a cell, acclimatethe cantilever to the 37°C warm HBRS (this may take up to 1 h). As long as the vertical detection signal is not stable (more than ±0.01 V/s), you should not start your experiment.

8. Air bubbles may be seen at the cantilever in solution. To eliminate the air bubbles lift the BioScope head and dry the cantilever with filter paper tissue (if necessary repeat this procedure "dry-wet" for a few times). Do not touch the cantilever and the tip; just hold the paper on the chip that carries the cantilevers.
9. Initial parameter settings are: scan size: 0 µm (during AFM tip approach), 1 µm (after successful AFM tip engagement); scan speed: 1 Hz, scan angle: 90°; integral gain: 3; proportional gain: 5; scan lines: 256, input attenuation: 8.
10. Bring the AFM tip in contact with the glass cover slip by using computer-controlled options.
11. After AFM tip engagement with the glass surface switch to the force calibration curve to calibrate the cantilever sensitivity (see manual for details). Measure your loading force. The loading force can be calculated by measuring the distance between the noncontact part of the force curve and the set-point line. This value (in nm) multiplied by the spring constant gives the loading force (for details, *see* Appendix). You should not exceed a loading force of 1 nN when working with living cells. Start with a loading force of 0.5 nN and then switch to the image mode. If the cantilever is in contact with the glass surface increase the integral and proportional gains until the piezos start oscillating. Decrease the integral and/or the proportional gain until oscillations stop. Gains should be as high as possible without piezo oscillations. If 0.5 nN is not sufficient to maintain the contact between cantilever and glass surface increase the loading force stepwise (+0.1 nN steps) and repeat gain settings. Good values are: loading force below 1 nN, an integral gain above 3, and proportional gain above 5. After each single image switch to the force calibration mode to see whether the loading force is constant. A constant force curve is reflected by the same loading force at a given set point. Another way to test the stability of your loading force is to look at the vertical movement of your force calibration curve. A small vertical movement of the force calibration curve (approx 0.01 nN/min) cannot be avoided (because of thermal drift).
12. After getting reproducible and stable images (no piezo oscillations and a small cantilever drift) on glass (no cells), store a force curve and an image. Lift the BioScope head and replace the empty glass cover slip with a cover slip with cells.
13. The cantilever should be exchanged after each experimental session. Use only new cantilevers with clean AFM tips. When you are imaging living cells, you should put the cantilever chip under UV-light for several minutes to sterilize the tip before you mount it in the holder. A simple way to check if the tip is "dirty" is checking the quality of an image of the glass surface. Another possibility is to perform a force curve on glass. The force curve should show a sharp bend where it contacts the surface. A shallow transition from the noncontact part to the contact part is a hint that the tip has picked up some soft junk. It is a good idea to use a new cantilever for a new day you are doing experiments.
14. To clean the cantilever holder just use distilled water and soap. Dry the holder in a nitrogen jet stream. Be careful not to scratch the holder. Before you mount a new cantilever, the holder has to be dry.

3.3. EC Preparation for AFM

1. Isolate HUVECs and grow in culture as described *(27)*. For experiments, we use confluent endothelial cells not older than 14 days (passage 1) cultured on a thick (1 mm) glass cover slip (Important: a thick glass cover slip reduces glass vibrations during scanning).
2. Cells are washed with 37°C HBRS to clean the surface of cell debris.
3. The glass cover slip must be mounted firmly in the perfusion chamber. We use Superglue (Uhu GmbH, Bühl, Germany) to fix the glass cover slip in the chamber. For firm gluing, it might be necessary to dry the bottom of cover slip. Take care to ensure that cells never get dry. After glass cover slip fixation, start superfusion with 37°C HEPES-buffered solution (flow velocity: 1–5 mL/min). Cells are bathed in about 2 mL of solution. Alternatively, you can culture cells in a Petri dish, which can be mounted in the perfusion chamber. Make sure that the fluid level is not too high in order to avoid salt solution creeping into the piezos of the AFM head (*see* manual for details).

3.4. Single-Cell Volume Measurement in a Living Cell

1. Bring the cantilever close to the cell and allow adaptation to the 37°C warm HBRS. Start the perfusion. To avoid thermal fluctuations heat the perfusion chamber (37°C) and the solutions to 37°C. It may be even helpful to warm up your whole equipment in the box (approx 30°C).
2. To get a good image of your cells keep the loading force as low as possible. Therefore, follow the first contact between the cantilever and the cell immediately with force calibration. Initial parameter settings are as follows:
   scan size: initially 0 µm (approach), then (after contact) increase to 1 µm; scan speed: 1 Hz; scan angle: 90°;integral gain: 3; proportional gain: 5; input attenuation: 8; scan lines: 256; no offline plane fit or flattening!
3. After the AFM tip engages the cell surface (**Fig. 1**), switch to the force calibration curve to measure the loading force. Do not exceed a loading force of 1 nN. Start with a loading force of 0.5 nN and then switch to the image. When the cantilever is in contact with the cell surface, increase the integral and proportional gains until piezo oscillations occur. Then, decrease gains slightly. If 0.5 nN is not sufficient to keep the contact between cantilever and cell surface increase the loading force step by step (+0.1-nN steps).
4. After obtaining a reproducible image try to increase the scan size (in 10-µm steps) up to 50 µm. You may have to increase the loading force by 0.1–0.3 nN. Now you should see a whole cell appearing on the screen (**Figs. 2** and **3**). Then you may increase the scan size to 100 µm for imaging larger areas. For an accurate volume analysis in the offline mode (*see* **Subheading 3.7.**) you need to have a small glass area as a reference level in your image. It should be visible between the cells. Thus, use a subconfluent cell monolayer. Over the entire course of the experiment, always try to reduce the loading force by decreasing the set point. As soon as you loose contact with the cell surface increase the set point until contact

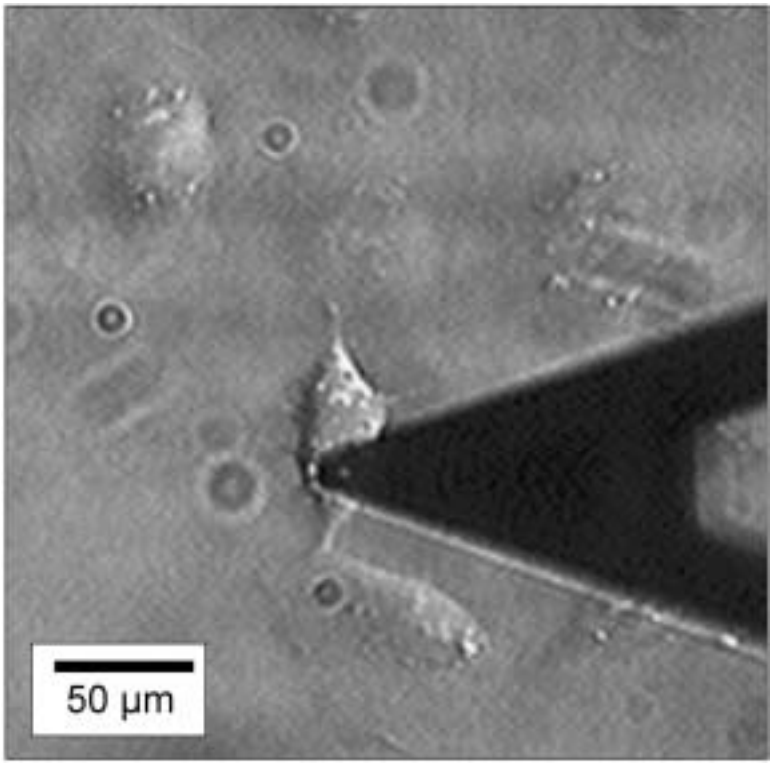

Fig. 1. Light microscopy image showing the cantilever located above the plasma membrane of a living cell. Scanning occurs in parallel to the longitudinal cell axis.

is restored. After using the lowest possible loading force try to increase the integral and proportional gain until the piezos start oscillating. Try to increase your scan speed to 2 Hz. Scan speed is also limited by piezo oscillations.

5. If the piezo reaches its limits, use the step motor function and retract the piezo from the surface (0.5-µm steps). The piezo should be almost completely extended when the AFM tip is scanning the glass substrate. To achieve this, move the AFM-tip to a cell-free site on the glass cover slip and adjust the scan offset values. Set the scan size to zero. The piezo should be completely extended. (Check the white bar in piezo position.)
6. Store the images. Control the loading force after each image.
7. Before switching to the aldosterone solution, store the force calibration curve.
8. To measure cell swelling upon aldosterone stimulation switch to a perfusion solution containing 1 n*M* aldosterone (**Fig. 2**). One image takes about 2–4 min (*see* **Notes 1–6**). So, before switching to an aldosterone-containing solution, make sure that you activate the movie capture mode (images will be continuously stored). Do not forget to store force calibrations curves.

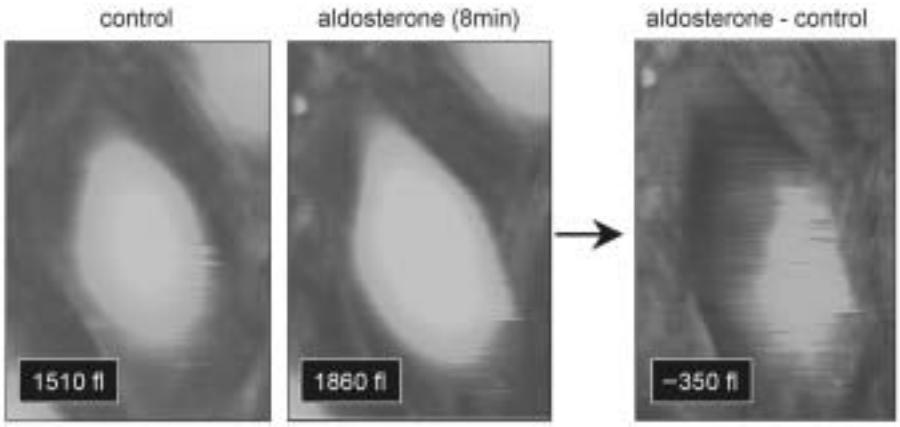

Fig. 2. Rapid endothelial cell swelling in response to aldosterone. One living EC is visible. Different brightness relates to different heights within the cells. After addition of aldosterone, the EC volume increases within 8 min. The cell changes its morphology because of the volume increase, shown by a change of the brightness pattern. Subtraction image (aldosterone – control) shows localized cell swelling within the cell (net volume change). Note that cell swelling occurs where the cell nucleus is located. This is typical for steroid hormone action.

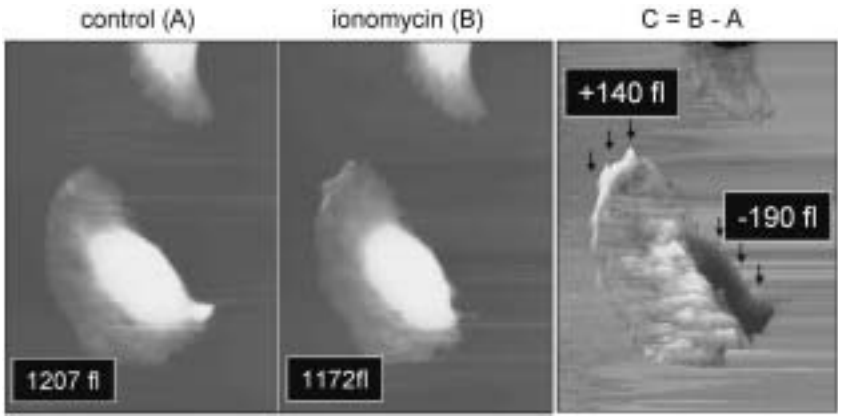

Fig. 3. Cell volume measurement in a migrating transformed kidney (Madin-Darby canine kidney [MDCK]) cell (migration direction: to upper left corner) before **(A)** and after **(B)** addition of ionomycin. Ionomycin increases intracellular calcium and thereby activates a potassium channel at the rear end of the cell and the Na^+/H^+ exchanger at the lamellipodium (front of the cell). The Na^+/H^+ exchanger activity increases cell volume. The potassium channel decreases cell volume. Image C represents the net volume change (volume increase at the front and volume decrease at the rear end of the cell) by subtracting both images (**C = B – A**).

9. After about 15–30 min, switch back to the control solution, store the images, and then stop the experiment.
10. Calibrate the cantilever again on glass (see **step 5**). Compare the sensitivities. If sensitivity is different at the end of your experiment compared with the initial sensitivity value take the mean value of both to calculate the loading force of the past experiment.

3.5. Single-Cell Volume Measurement in a Nonliving, Fixed Cell

In addition to cell volume measurements on living cells, it is also possible to image and analyze the volume of fixed cells (**Fig. 4**). Fixed cells are much easier to measure because of there is an increase in stiffness after fixation (higher resolution, less indentation by the loading force), the work can be done at room temperature, and cell activity, such as migration, is eliminated. However, paired experiments are not possible as well as the continuous monitoring of volume fluctuations. Moreover, fixation may cause volume and topography artifacts. For cell fixation we use 4% paraformaldehyde dissolved in 100 m*M* sodium-phosphate supplemented with 4% sucrose; pH 7.4; incubation time is 12 h at 4°C. After fixation cells are washed with 100 m*M* sodium phosphate buffer with 4% sucrose (personal communication by R. Ossig). Always keep cells under fluid. Mounting the glass cover slip in the perfusion chamber and imaging procedures are identical to the one described in **Subheading 3.4.**. It is not necessary to work at 37°C and under constant buffer perfusion, reducing electrical, mechanical, and thermal noise. For further fixation protocols, check *Current Protocols in Cell Biology* ***(29)***.

3.6. Visualization of Local Intracellular Volume

To visualize the local volume change upon stimulation of a single living cell you can subtract two subsequent images from each other. You have to make sure that in both images the scan area and cell localization within this area are identical. Go into the browse menu, select the two images and subtract them from each other. The new image shows the "net volume" change within a single cell. In case of localized volume changes you can detect intracellular compartments that undergo volume changes (**Figs. 2** and **3**).

3.7. Single-Cell Volume Off-Line Analysis

Cell volume analysis is based on the following principle: Each pixel includes information on three dimensions (i.e., on *x*, *y*, and *z* axes). The *x* and *y* parameters are given by the size of the scan area and by the number of scan lines per image. The *z* (height) information is given by the specific gray level of each pixel.

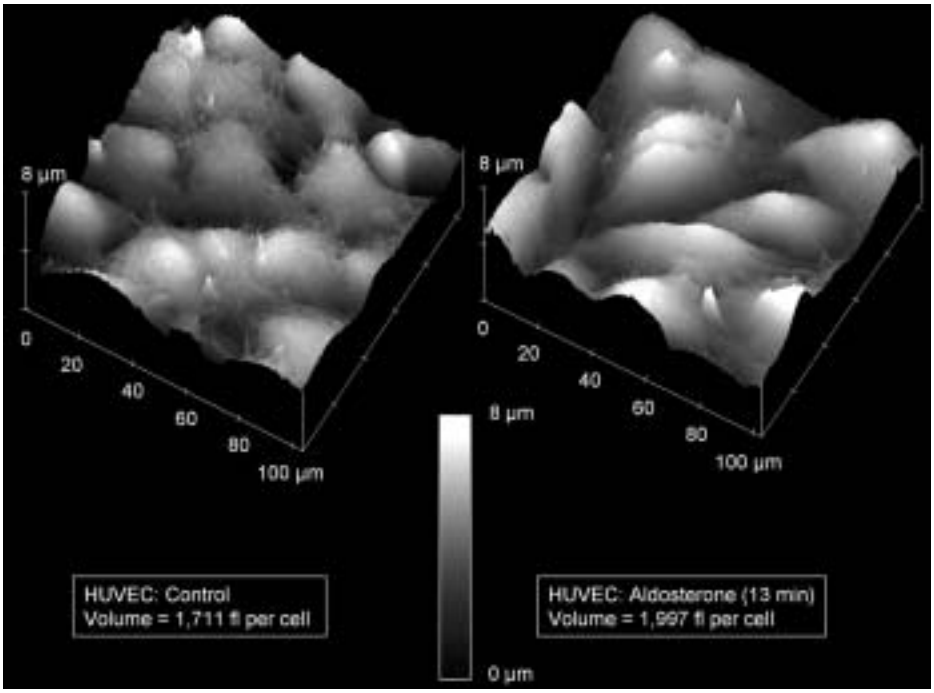

Fig. 4. Fixed endothelial cells (HUVEC) imaged in fluid in the absence (control) and 13 min after addition of aldosterone. Cells are grown on gelatin-coated glass and fixed in physiological conditions directly in the incubator, i.e. in culture medium supplemented with serum at 5% CO_2 at 37°C. Fixation was performed by gently adding the fixative (glutaraldehyde) to the cells to reach a final concentration of 0.5%.

1. Bring the image into a "correct" horizontal plane by using plane fit, order one. Glass surface visible between the endothelial cells helps to show if the cell layer is in a correct horizontal position.
2. The software provides an analysis tool "bearing" (**Fig. 5**). Drawing a square on the image gives the total volume (μm^3, equivalent to 10^{-15} L or 1 fL) inside the square. Move the marker (triangle) in the bearing area graph to 100%. The software uses the lowest point in the image as a reference for volume calculation. The best reference level is the glass surface.

3.8. CAVE

For contact mode imaging, it is necessary to apply a (minimal) loading force to the cell. Because cells are soft, it is unavoidable that plasma membranes will be indented by the AFM tip, even if the loading force is at the minimum necessary for successful contact mode imaging. This indentation

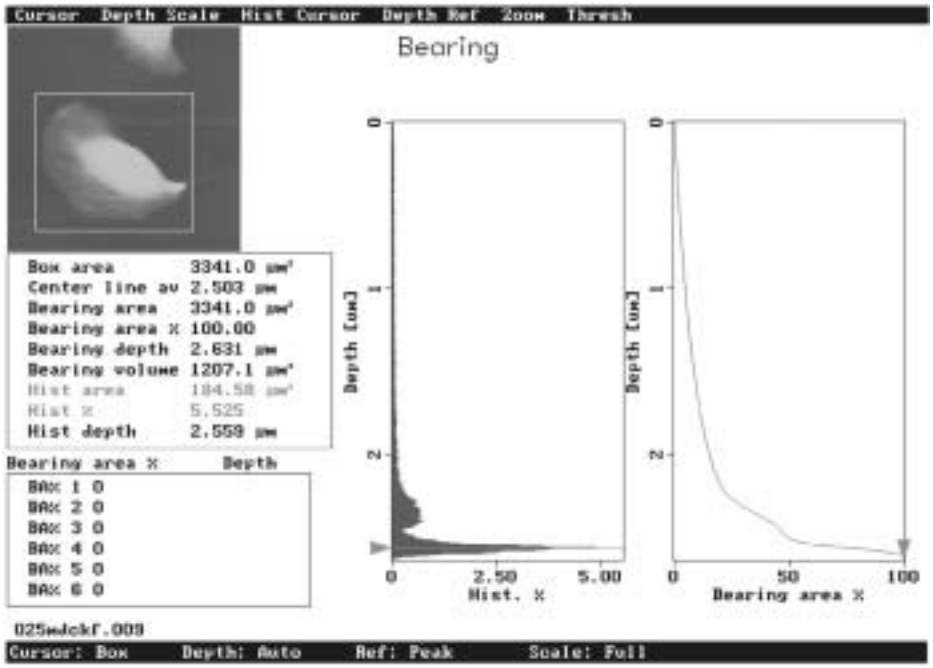

Fig. 5. Single-cell volume offline analysis. Using the bearing feature of the software package, it is possible to measure single-cell volume (1 μm^3 = 1 fL). The white box in the image limits the area used for volume calculations. Draw the box around the cell including the substrate (i.e., glass) to have a reference level. Displace the marker (triangle) in the bearing area graph to 100%. The volume is given as bearing volume in μm^3. The cell volume of the presented example is 1207 fL. In addition to cell volume calculation the program provides a height histogram (Depth [µm] vs Hist. %).

leads to an underestimation of the cell height and therefore to an underestimation of the cell volume. The physical parameter that describes the stiffness of a material is the elastic modulus E (also called Young's modulus). Typical values for living cells are 1–10 kPa , for fixed cells, 10–100 kPa. (Compare with rubber: 1.5 MPa; with glass: 1 GPa; **ref. *30***). For example: a loading force of 0.5 nN applied to a cell with a Young's modulus of 5 kPa causes a cell indentation of 400 nm. If we propose an actual cell height of 4 µm, the volume measurements in contact mode underestimate the cell volume by about 10% (**Fig. 6**). The indentation varies also strongly with the applied loading force. Therefore, it is necessary to keep the loading force constant to obtain reliable volume measurements.

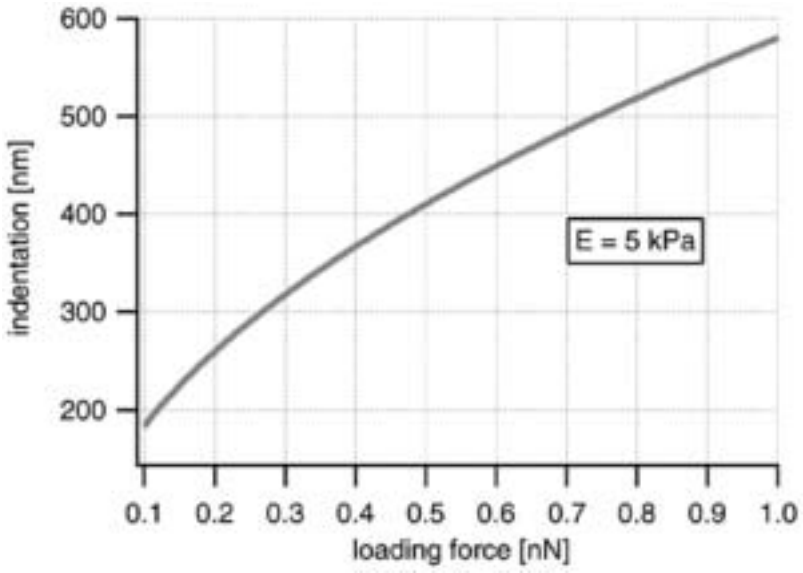

Fig. 6. Indentation of a soft sample with an elastic modulus of E = 5 kPa (a typical value for living cells) as a function of the applied loading force for the geometry of a typical AFM tip. Typical loading forces (several 100 pN) used for contact mode imaging cause indentations from 200 to 600 nm. Because the height of cells is in the range of only a few micrometers (typical value 4 μm), such indentations are significant. The indentation also varies strongly with the loading force. Therefore, it is necessary to keep the loading force constant to obtain reliable volume measurements. The Hertz model for a conical indenter with a half opening angle of 35° was used for this calculation.

Another problem is that the biochemical stimulus used to change the cell volume might also change the elastic properties of the cell. Such changes will also change the indentation, even if the loading force is kept constant (**Fig. 7**). Because of the elastic indentation of the cell by the AFM tip, cell volume measurements in contact mode lead to an underestimation of the absolute cell volume. However, relative changes can be measured if the loading force is constant during the measurement and if the elastic properties of the cell do not change. As long as these parameters remain constant volume underestimation is a systematic error and relative volume changes upon cell stimulation are virtually correct.

In practice, it is not easy to keep the loading force constant because thermal fluctuations cause a bending of the cantilever and therefore alter the force. This bending is caused by the bimetallic construction of the cantilever and even very small changes in temperature can change the loading force by several

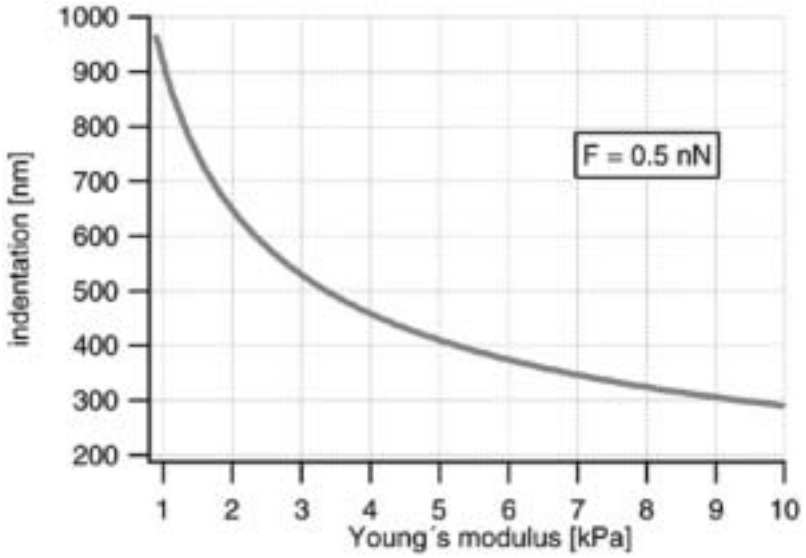

Fig. 7. Indentation of a soft sample at a constant loading force of 0.5 nN as a function of the elastic modulus of the sample. The Hertz model for a conical indenter with a half opening angle of 35° was used for this calculation.

hundred pN, a change that alters the indentation significantly (**Fig. 6**). Another consideration is that changes in cell elasticity may occur that will change the indentation significantly (**Fig. 7**). For example, the stimulation of endothelial cells with thrombin (a mediator of inflammation that increases the permeability of the endothelial monolayer) changes the cell elasticity by a factor of 5 (unpublished data by R. Matzke). A third point is that it is desirable to obtain quantitative volume data. A method to circumvent the above mentioned problems is to operate the AFM in the force-mapping mode (also called force-volume mode; **ref. *31***). This method allows a quantification of the unindented cell volume, independent of the loading force and independent of the elastic modulus of the cell. It allows a measurement and quantification of the local cell elasticity. The BioScope can be operated in the force volume mode. Therefore, it would be possible to calculate actual cell height and cell volume irrespective of cell stiffness. The BioScope software permits a qualitative analysis of the elastic properties of the sample, but features to calculate the unindented height and to quantify the elastic modulus are missing. In other words, it is possible to record all the data necessary for a actual cell volume measurement, but we cannot analyze the data with the current BioScope software. A group of researchers, M. Radmacher, C. Rotsch and R. Matzke (Departments of Physics; Universities of Munich and Göttingen, Germany) wrote a program in IGOR

PRO (Wavemetrics, Lake Oswego, OR) to analyze the force volume data. Please, check the Appendix and the literature ***(30–36)*** for further information.

3.9. Appendix

Force Mapping ***(31)*** allows a quantification of the unindented cell volume, independent of the loading force and independent of the elastic modulus of the cell. The following section explains the analysis of the data and gives practical hints for data acquisition.

3.9.1 Force Mapping

A force map is a 2D array of force curves. (You already know a single force curve from the force calibration menu of the BioScope.) In a force curve, the force acting on the AFM tip is measured as the tip approaches and retracts from the surface of a sample (**Fig. 8**). Typically, the cantilever starts the approach from a point where it is not in contact with the surface. After contact, it can be further approached until a maximal loading force is reached. Then the cantilever is retracted from the surface until the tip is free again. The deflection and the vertical position of the z piezo are recorded in such a force curve. According to Hooke's law, the loading force, F, can be calculated by multiplying the measured deflection, d, with the spring constant, k_C, of the cantilever.

$$F = k_C \times d \tag{1}$$

A force curve consists of two parts: the noncontact part and the contact part. When the tip is not in contact with the surface, the deflection will be constant. A further motion down after contact will deflect the cantilever. On a stiff sample, this deflection is equal to the travel of the z piezo after the contact point because the stiff sample cannot be indented (**Fig. 8**). However, a soft sample will be indented by the tip. Thus, the force curve will be shallower than on a stiff sample (**Fig. 9**). The indentation, $\wp$, at a certain loading force can be calculated as the travel of the z piezo, z, after the contact point minus the deflection of the cantilever.

$$\wp = z - d \tag{2}$$

The unindented height of the sample can be calculated by finding the contact point. The contact point can be found rather easily in the case of a stiff sample since the force curve shows a sharp bend there (**Figs. 8** and **9**). In the case of a soft sample, the exact position of the contact point is often hard to determine since the transition between noncontact part and contact part is very shallow (**Fig. 9**). The contact point may also be hidden by thermal noise. A method to determine the contact point on a soft sample is described below. From the contact part of a force curve the elastic modulus can be calculated

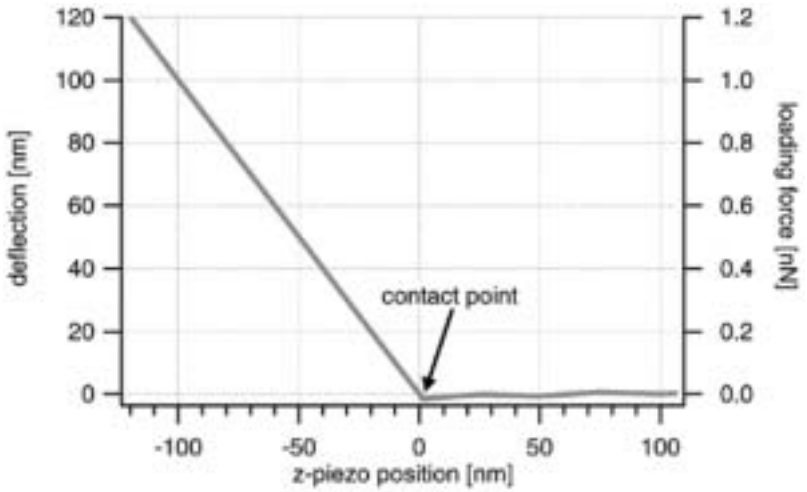

Fig. 8. Force curve on a stiff sample. Only the approach part is shown. The force curve consists of two parts: the noncontact part and the contact part. As long as the tip is not in contact with the surface, the deflection (and therefore the loading force) is constant. The tip contacts the surface in the contact point. In the contact part, a further approach deflects the cantilever. Because the stiff sample cannot be indented by the tip, the deflection equals the travel of the z piezo after the contact point.

by analyzing the force dependent indentation. This analysis will also be described below.

By recording a 2D array of force curves on a cell, a map of the unindented height and a map of the local elastic properties can be calculated (**Fig. 10**).

3.9.2. Calculation of the Contact Point and of the Elastic Modulus

The contact part of a force curve on a soft sample is nonlinear because the compliance of the sample becomes higher for larger loading forces. This is attributable to a geometrical effect. AFM tips are approximately conical and therefore the contact area increases with the increasing indentation. This process was treated analytically first by Hertz *(37)* and a more general solution was obtained by Sneddon *(38)*. For the geometry of a conical tip indenting a flat sample (which is most appropriate here) the relation between the indentation, $\wp$ and the loading force, F, is given by the following:

$$F = \wp^2 \times (2/\Theta) \times (E/[1-\downarrow^2]) \times \tan(\diagup) \quad (3)$$

where $\downarrow$ is the Poisson ratio, E is the elastic modulus, and $\diagup$ is the half opening angle of the conical tip. For incompressible materials (as assumed for cells), the Poisson ratio is 0.5. The half opening angle for Microlever (Park Scien-

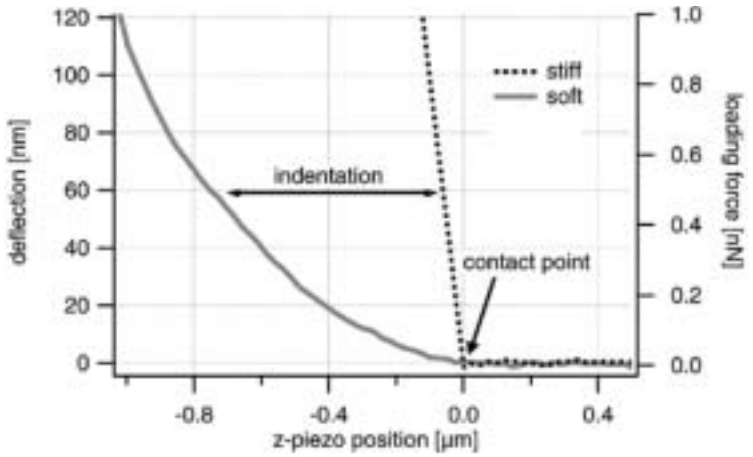

Fig. 9. Force curves on a soft and on a stiff sample. Only the approach parts are shown. The curve on the soft sample is shallower because sample is indented by the tip. The indentation is the travel of the z piezo after the contact point minus the deflection. The curve is nonlinear because the compliance becomes higher for larger loading forces. This is the result of a geometrical effect: AFM tips are (approximately) conical and therefore the contact area increases with the indentation. The contact point can very easily be determined on the stiff sample since the force curve shows a sharp bend there. On the soft sample, the determination of the contact point is more difficult since the transition between noncontact part and contact part is very shallow. *See* text for how to find the contact point on a soft sample.

tific) is 35°. The loading force can be calculated by **Eq. 1** and the indentation can be calculated by **Eq. 2**. This gives the following:

$$k_c \times d = (z - d)^2 \times (2/\Theta) \times (E/[1 - \downarrow^2]) \times \tan(\diagup) \quad (4)$$

Thus, the elastic modulus can be calculated by the measured deflection and z-piezo position. However, in measured data the deflection of the noncontact part of the force curve is not necessarily zero (**Fig. 11**). Therefore, the deflection, d, must be replaced by the following:

$$d\,\gamma \quad d_i - d_0 \quad (5)$$

where d_0 is the deflection offset and d_i is a measured deflection value.

Eq. 3 is only valid for the contact part of the force curve. Thus, the contact point z_0 must be subtracted from a measured z-piezo value, z_i. Because the BioScope® stores force curves inverted (i.e., the point with the maximal deflection has the z-value 0 and the starting point of the approach has the maximum z value, **Fig. 11**), z must be replaced by the following:

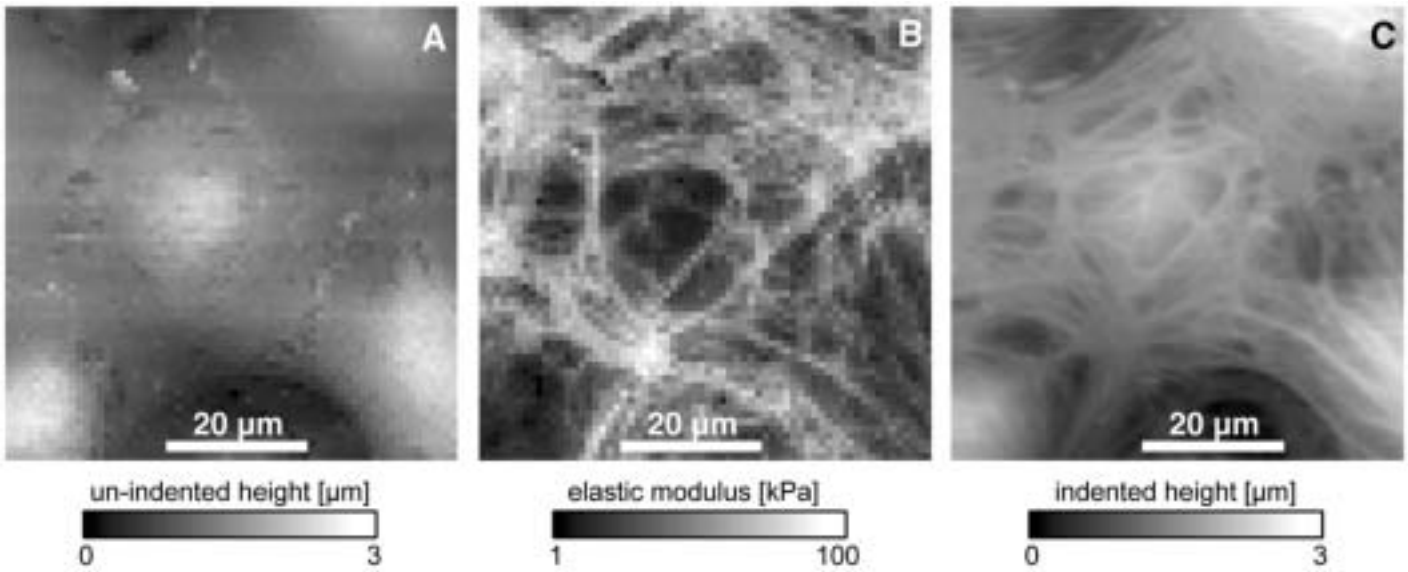

Fig. 10. Force maps of a living endothelial cell (HUVEC). **(A)** unindented height, **(B)** elastic modulus, and **(C)** contact mode image of the same cell. The unindented height image **(A)** shows a smooth cell surface, whereas the contact mode image shows height fluctuations **(C)**. This is because the indentation depends on the local elastic properties; soft regions will be more indented than stiffer regions. The cytoskeleton is a structured polymeric network with very different local elastic properties, as shown in the elasticity map **(B)**. The elastic indentation leads to an underestimation of the cell volume.

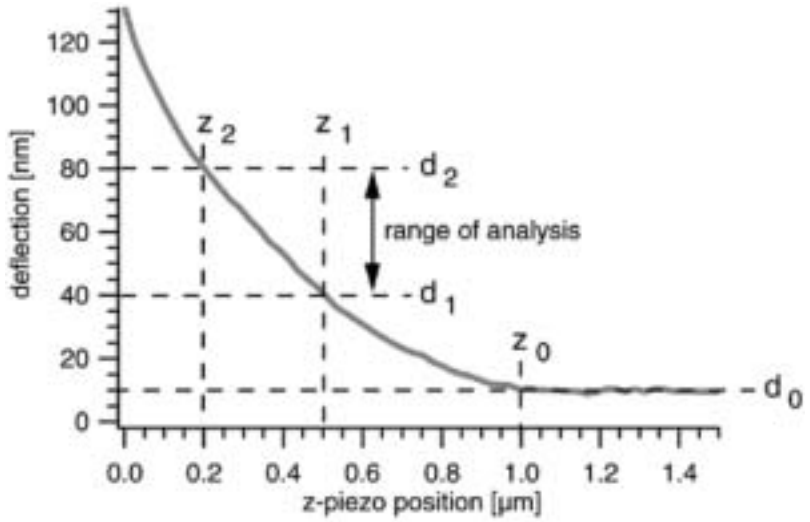

Fig.11. Parameters used for the calculation of the contact point and the elastic modulus. The two deflection values d_1 and d_2 and their corresponding z-piezo positions z_1 and z_2 define the range of analysis. The deflection-offset d_0 is given by the noncontact part of the force curve. With these values and **Eqs. 9** and **10**, the contact point z_0 and the elastic modulus can be calculated. In this example, $d_0 = 10$ nm, $d_1 = 40$ nm, $d_2 = 80$ nm, $z_1 = 0.5$ µm, $z_2 = 0.2$ µm, and $z_0 = 1$ µm.

$$z \gamma \quad z_o - z_i \tag{6}$$

where z_0 is the z-piezo value of the contact point and z_i is a measured z-piezo position value (**Fig. 11**).

Eqs. 5 and **6** inserted in **Eq. 4** gives the following:

$$k_c \times (d_i - d_0) = [(z_0 - z_i) - (d_i - d_0)]^2 \times (2/\Theta) \times [E/(1 - \downarrow^2)] \times \tan(\swarrow) \tag{7}$$

In this equation, we have three unknown parameters: the deflection offset, d_0, the contact point, z_0, and the elastic modulus, E. The deflection offset can easily be determined by the noncontact part of the force curve. As mentioned above, the transition from noncontact to contact part is very shallow and therefore the contact point cannot be determined by easy means. Unfortunately, **Eq. 7** is of such a form that an analytical least squares fit to determine E and z_0 cannot be performed. One possibility is to perform a Monte-Carlo fit with reasonable starting values. However, the two missing parameters can be obtained more easily.Since the signal-to-noise ratio of measured data is very good (because thermal noise is reduced when the tip contacts the cell), we can

take two measured deflection values, d_1 and d_2, and their corresponding z-piezo values, z_1 and z_2, of the contact part of the force curve and insert them in **Eq. 7**. This gives two equations with two missing parameters, E and z_0:

$$k_c \times (d_1 - d_0) = [(z_0 - z_1) - (d_1 - d_0)]^2 \times (2/\Theta) \times [E/(1 - \nu^2)] \times \tan(\alpha) \quad (8a)$$

$$k_c \times (d_2 - d_0) = [(z_0 - z_2) - (d_2 - d_0)]^2 \times (2/\Theta) \times [E/(1 - \nu^2)] \times \tan(\alpha) \quad (8b)$$

The contact point can be calculated by solving Eq. 8a for E and inserting E in Eq. 8b:

$$z_0 = \frac{(z_2 + d_2)\sqrt{d_1} - (z_1 + d_1)\sqrt{d_2}}{\sqrt{d_1} - \sqrt{d_2}} \quad (9)$$

The elastic modulus can now be calculated by inserting z_0 in Eq. 8a or 8b.

A better method to calculate the elastic modulus is to apply an analytical least squares fit (this is possible now because z_0 is known) to all the data points (d_i/z_i) in the range of analysis (**Fig. 11**) that is limited by (d_1/z_1) and (d_2/z_2):

$$E = \frac{\sum_1 F_i \wp^2}{\sum_1 \wp^4} \times \frac{\Theta \cdot (1 - \nu^2)}{2 \cdot \tan(\alpha)} \quad (10)$$

where $\wp = (z_0 - z_i) - (d_i - d_0)$.

The BioScope stores force curves in the force volume mode in a relative manner. This means that the absolute position of the z piezo is not recorded in the force curve itself and every force curve starts with $z = 0$. The force volume data consists of two separate datasets, one that contains the array of force curves, and another, in which the absolute height information is stored. Each pixel of the height image represents the absolute z-piezo value when the corresponding force curve switches from approach to retract (i.e., the point with the maximal loading force). Therefore, to calculate the unindented height, H_0, we have to add the calculated contact point, z_0, to the height at maximal loading force, H:

$$H_0 = H + z_0 \quad (11)$$

3.9.3. How to Access the Force Volume Data from the BioScope File

A force volume measurement consists typically of 64 × 64 force curves. Because of the amount of data, it is convenient to write a computer algorithm to analyze the data. Unfortunately, the BioScope software cannot export force volume data in a standard data format like ASCII. However, there is data analysis software (like IGOR PRO) that can read the binary information of the BioScope data file. At this time, it is difficult to give general advice on how to reconstruct the data from the binary file since the file format has changed in the past rather frequently for the various BioScope software versions. Please refer

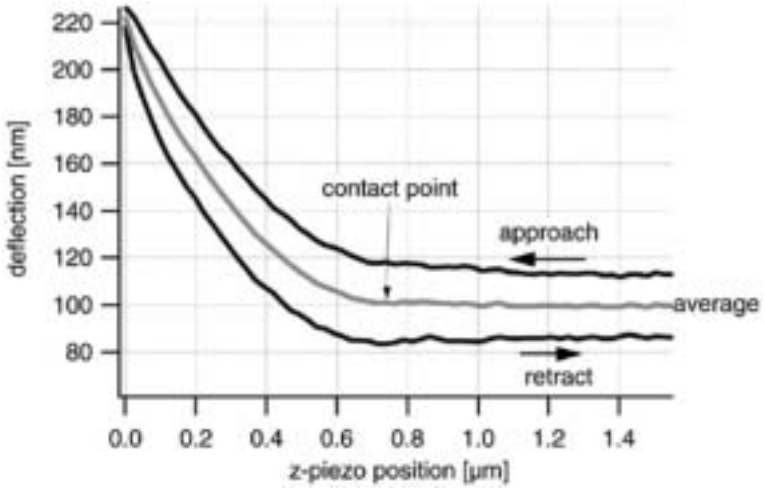

Fig. 12. Force curve on a living cell in liquid medium. The approach and retract parts are separated by hydrodynamic drag that adds a constant external force to the loading force of the cantilever. This force-offset is speed dependent (the faster the scan speed the bigger the force-offset; data not shown here) and changes its sign when the direction of movement is reversed from approach to retract. One way to deal with this force-offset is to average the approach and retract part point by point and to analyze the resulting average force curve.

to the manual of your software version to get information about the file and data structure.

When you are measuring living cells, the AFM is operated in liquid. In this case, the approach and retract part of the force curves are separated from each other (**Fig. 12**). This separation is caused by hydrodynamic forces as the cantilever is dragged through the fluid medium ***(34)***. This causes a force offset that depends on the speed of the z piezo, and the sign of that offset changes when the direction of movement is reversed between approach and retract. One way of dealing with this force offset is to average point by point the approach and retract part of the force curve and use this average for further analysis.

3.9.3.1 Notes

The Hertz model applied in the analysis is valid on condition that the sample is thick compared with the indentation, is homogeneous, and is flat, and that the geometry of the tip is a cone. The real situation fits these requirements only partly. The typical height of cells in the region of the nucleus is 4 µm. Here the height is sufficiently large versus the indentation (approx 400 nm). In the region of the thin lamellipodium, this condition is not fulfilled. With increasing indentation, the tip will feel the underlying stiff substrate and the force curve

will be initially the shape of a curve for a soft sample, but it will become linear and appear like a curve for a stiff substrate at higher deflection values ***(36)***. For the analysis of force curves taken on thin cell regions, it is therefore necessary to choose a fit range with sufficiently small deflection values ***(32)***. At small indentation values, the geometry of the AFM tip on nano-meter scale will become important. AFM tips look like a pyramid whose top is formed by a half sphere. The radius of that sphere is typically in the range of 50 nm. The Hertz model for the cone is no longer appropriate here. A better description of the data is the Hertz model for a sphere indenting a flat surface:

$$F = \frac{4}{3} \times \frac{E}{1 - \nu^2} \times \delta^{3/2} \times \sqrt{R} \tag{12}$$

where R is the radius of the tip ***(35)***.

Because the area of the cell surface is large, compared to the radius of the tip, one can assume as an approximation that the sample is flat, and thereby satisfy the Hertz model.

Cell material is not at all homogeneous. The cytoskeleton is a polymeric network that consists of polymers with very different elastic properties. There might also be contributions to the measured elastic modulus from the lipid membrane or from tension in the cytoskeleton. However, the scope of this article is the determination of the cell volume and not the quantification of the elastic modulus. Inhomogenieties may lead to an apparent elastic modulus, i.e., an average of all elastic components that contribute to the measured value. In practice, the contact point can be determined with sufficient precision despite this problem. If the elastic modulus changes with the depth of indentation (as with thin lamellipodia where the tip "feels" the underlying stiff substrate or when the elastic properties vary with the depth of indentation), one should take care that the data are analyzed in a fit range with small deflection values. Jan Domke (unpublished observation) showed by calculating simulations that the analysis of the cell height with the Hertz model gives reasonable values. There is only a systematic underestimation in the order of the tip radius.

3.9.4. How to Record a Force Map

Typical settings are trigger mode: relative; trigger threshold: 100 nm; z-scan size: 1.5 µm; z-scan speed: 10 Hz; 64 points per force curve, 64 × 64 points per image.

3.9.4.1 Comments

"Trigger mode: relative" means that the tip is approached to the sample until the cantilever reaches a deflection of "trigger threshold" (in our example 100 nm), relative to the deflection offset of the force curve given by the noncontact

part of the curve. This ensures that the deflection (and therefore the loading force) does not exceed the value given by trigger threshold. This prevents cell damage caused by high loading forces and ensures that the contact part of the scan will be long enough to find good deflection values for the data analysis. You can compare the relative trigger threshold with the set point in the contact mode, where the loading force can be adjusted by the set point. For the determination of the deflection offset, the force curve must contain a clear noncontact part (typically one-fourth of the total length of the force curve). In the BioScope, the tip is being approached until the deflection equals the trigger threshold. Then the z piezo moves upward the length given by the z-scan size. To get a distinct noncontact part, the z-scan size must be long enough for the tip to become free. A good starting value is 1.5 µm on living cells. With high cells, it might be difficult (or even impossible) to measure the topmost region of the cell since the necessary piezo travel range of the BioScope (6 µm) might be smaller than the height of the cell plus the z-scan range. New BioScope versions offer piezos with extended range. The z-scan speed is limited since hydrodynamic drag will cause a speed-dependent force offset. On the other hand, slow scan speed increases the time necessary to record a complete force map. A good compromise is a scan speed of 10 Hz. It will then take about 13 min to record a force map with 64 × 64 pixels. The number of pixels determines the lateral resolution. Of course, a small number will speed up data acquisition but decrease lateral resolution. However, you should consider the motion of the tip in the force-mapping mode: after recording one force curve, the tip moves laterally to record the next force curve. The lateral step size is given by the total lateral scan size divided by the number of pixels. With large step sizes, it might happen that the tip or cantilever bumps against the cell when it moves to the side because the tip is not far enough above the cell than the height of the cell increases. If possible, you can either increase the z-scan size or increase the number of pixels. Note that the BioScope cannot store more than 64 × 64 × 64 data points (64 lines × 64 columns × 64 points in the force curve). When you increase the length of the force curve, the force resolution of the curve will become worse. Smaller lateral pixel numbers permit more points in the force curve (for example, 16 × 16 × 512).

4. Notes

1. How to increase your time resolution: If it is not necessary to record all three dimensions (*x*-, *y*-, and *z*-axis) of the cell you can increase time resolution (up to 100 ms/line) by imaging only two dimensions (*x*- and *z*-axis). Switch the mode from slow axis enable to slow axis disable (= line scan) in your software menu. The cantilever is now moving back and forth along the same scanning line (*x*-axis). The *y*-axis will not be recorded. Fast volume fluctuations upon cell stimulation are now visible as a height increase or decrease.

2. Before starting cell imaging, make sure that your system provides good and stable images on a clean glass cover slip under fluid. This will help you to distinguish between problems that arise from the microscope (AFM tip damaged, air bubbles stuck to the cantilever, mechanical vibrations) or problems caused by the cells (membrane blebbing, cell detachment, etc.).
3. ECs that are under scanning should not change their morphology. You can observe the cells constantly through the light microscope.
4. The temperature of the environment (in the box) should be close to 37°C (in practice: approx 30°C) to minimize temperature alterations. Any increase or decrease of the temperature in the bath solution (which must have 37°C) is followed by artificial cantilever deflections.
5. Avoid acoustical or mechanical noise (speaking or walking) during the experiment.
6. If you cannot get an image or if you cannot increase the integral gain above 1 and the proportional gain above 2, check or modify the following parameters:
   a. Increase the loading force.
   b. The glass cover slip is too thin (<0.8 mm);
   c. There is a lot of noise or vibrations in your laboratory. Switch off: heating chamber, microscopy lamps, perfusion system, etc. Install the BioScope computer some distance away from the scanner and make sure that its fan does not blow in the direction of the scanner;
   d. The temperature of the bath solution is not constant;
   e. There are air bubbles stuck to the cantilever;
   f. The AFM tip is dirty;
   g. The cells detach from the glass surface (e.g., temperature above 37°C);
   h. The cells show membrane blebbing (a hint that the cells are in a bad condition and/or get damaged by the scanning tip);
   i. The glass cover slip (with the cell layer) is not firmly fixed in the perfusion chamber and thus comes off;
   j. Cell height is beyond the *z* piezo range of the instrument. Decrease the scan size or try to image a flat cell surface area (i.e. lamellipodium or cell–cell contact area). Adjust the piezo height with the step motor.

Acknowledgments

This work was supported by the VW-Stiftung (AZ I/77299) and the Interdisziplinäre Zentrum für Klinische Forschung (IZKF, TP I/90).

References

1. Harvey, B. J. , Condliffe, S., and Doolan, C. M. (2001) Sex and salt hormones: rapid effects in epithelia. *News Physiol. Sci.* **16,** 174–177.
2. Wehling, M., Käsmayr, J., and Theisen, K. (1991) Rapid effects of mineralocorticoids on sodium exchanger: Genomic or nongenomic pathways? *Am. J. Physiol.* **260,** E719–E726.
3. Wehling, M., Ulsenheimer, A., Schneider, M., Neylon, C., and Christ, M. (1994) Rapid effects of aldosterone on free intracellular calcium in vascular smooth

muscle and endothelial cells: subcellular localization of calcium elevations by single cell imaging. *Biochem. Biophys. Res. Commun.* **204,** 475–481.
4. Gekle, M., Silbernagl, S., and Oberleithner, H. (1997) The mineralocorticoid aldosterone activates a proton conductance in cultured kidney cells. *Am. J. Physiol.* **273,** C1673–C1678
5. Schneider, S. W., Yano, Y., Sumpio, B. E. , et al. (1997) Rapid aldosterone-induced cell volume increase of endothelial cells measured by the atomic force microscope. *Cell Biol. Int.* **21,** 759–768.
6. Vaupel, P., Kelleher, D. K., and Hockel, M. (2001) Oxygen status of malignant tumors: pathogenesis of hypoxia and significance for tumor therapy. *Semin. Oncol.* **28,** 29–35.
7. Winter, D. C., Schneider, M. F. , O'Sullivan, G. C. , Harvey, B. J., and Geibel, J. P. (1999) Rapid effects of aldosterone on sodium-hydrogen exchange in isolated colonic crypts. *J. Membr. Biol.* **170,** 17–26.
8. Urbach, V. and Harvey, B. J. (2001) Rapid and non-genomic reduction of intracellular [Ca(2+)] induced by aldosterone in human bronchial epithelium. *J. Physiol.* **537,** 267–275.
9. Oberleithner, H., Weigt, M., Westphale, H.-J., and Wang, W. (1987) Aldosterone activates Na+/H+ exchange and raises cytoplasmic pH in target cells of the amphibian kidney. *Proc. Natl. Acad. Sci. USA* **84,** 1464–1468.
10. Paccolat, M. P., Geering, K., Gaeggeler, H. P., and Rossier, B. C. (1987) Aldosterone regulation of Na+ transport and Na+-K+-ATPase in A6 cells: role of growth conditions. *Am. J. Physiol.* **252,** C468-C476
11. Schneider, S. W., Pagel, P., Storck, J., et al. (1998) Atomic force microscopy on living cells: aldosterone-induced localized cell swelling. *Kidney Blood Press. Res.* **21,** 256–258.
12. Cines, D. B., Pollak, E. S. , Buck, C. A., et al. (1998) Endothelial cells in physiology and in the pathophysiology of vascular disorders. *Blood* **91,** 3527–3561.
13. Phillips, P. G. and Tsan, M. F. (1988) Hyperoxia causes increased albumin permeability of cultured endothelial monolayers. *J. Appl. Physiol.* **64,** 1196–1202.
14. Shepard, J. M., Goderie, S. K., Brzyski, N., Del Vecchio, P. J. , Malik, A. B., and Kimelberg, H. K. (1987) Effects of alterations in endothelial cell volume on transendothelial albumin permeability. *J. Cell Physiol.* **133,** 389–394.
15. Barbee, K. A., Mundel, T., Lal, R., and Davies, P. F. (1995) Subcellular distribution of shear stress at the surface of flow- aligned and nonaligned endothelial monolayers. *Am. J. Physiol.* **268,** H1765–H1772.
16. Levin, E. G., Santell, L., and Saljooque, F. (1993) Hyperosmotic stress stimulates tissue plasminogen activator expression by a PKC-independent pathway. *Am. J. Physiol.* **265,** C387–C396.
17. Iba, T. and Sumpio, B. E. (1992) Tissue plasminogen activator expression in endothelial cells exposed to cyclic strain in vitro. *Cell Transplant.* **1,** 43–50.
18. Iba, T., Shin, T., Sonoda, T., Rosales, O., and Sumpio, B. E. (1991) Stimulation of endothelial secretion of tissue-type plasminogen activator by repetitive stretch. *J. Surg. Res.* **50,** 457–460.

19. Klein, J. D., Perry, P. B., and O'Neill, W. C. (1993) Regulation by cell volume of Na(+)-K(+)-2Cl- cotransport in vascular endothelial cells: role of protein phosphorylation. *J. Membr. Biol.* **132,** 243–252.
20. Marsh, D. J., Jensen, P. K., and Spring, K. R. (1985) Computer-based determination of size and shape in living cells. *J. Microsc.* **137,** 281–292.
21. Timbs, M. M. and Spring, K. R. (1996) Hydraulic properties of MDCK cell epithelium. *J. Membr. Biol.* **153,** 1–11.
22. Oberleithner, H., Brinckmann, E., Schwab, A., and Krohne, G. (1994) Imaging nuclear pores of aldosterone sensitive kidney cells by atomic force microscopy. *Proc. Natl. Acad. Sci. USA* **91,** 9784–9788.
23. Oberleithner, H., Giebisch, G., and Geibel, J. (1993) Imaging the lamellipodium of migrating epithelial cells in vivo by atomic force microscopy. *Pflügers Arch.* **425,** 506–510.
24. Radmacher, M., Tillmann, R. W., Fritz, M., and Gaub, H. E. (1992) From molecules to cells: imaging soft samples with the atomic force microscope. *Science* **257,** 1900–1905.
25. Schneider, S. W. (2001) Kiss and run mechanism in exocytosis. *J. Membr. Biol.* **181,** 67–76.
26. Schneider, S. W., Pagel, P., Rotsch, C., et al. (2000) Volume dynamics in migrating epithelial cells measured with atomic force microscopy. *Pflügers Arch.* **439,** 297–303.
27. Jaffe, E. A., Nachman, R. L., Becker, C. G., and Minick, C. R. (1973) Culture of human endothelial cells derived from umbilical veins. Identification by morphologic and immunologic criteria. *J. Clin. Invest.* **52,** 2745–2756.
28. Langer, F., Morys-Wortmann, C., Kusters, B., and Storck, J. (1999) Endothelial protease-activated receptor-2 induces tissue factor expression and von Willebrand factor release. *Br. J. Haematol.* **105,** 542–550.
29. Peters, P. J. (1999). Current protocols in cell biology 4.7.1–4.7.12, Wiley, New York.
30. Radmacher, M. (1997) Measuring the elastic properties of biological samples with the AFM. *IEEE Eng. Med. Biol. Mag.* **16,** 47–57.
31. Radmacher, M., Cleveland, J. P., Fritz, M., Hansma, H. G., and Hansma, P. K. (1994) Mapping interaction forces with the atomic force microscope. *Biophys. J.* **66,** 2159–2165.
32. Rotsch, C., Jacobson, K., and Radmacher, M. (1999) Dimensional and mechanical dynamics of active and stable edges in motile fibroblasts investigated by using atomic force microscopy. *Proc. Natl. Acad. Sci. USA* **96,** 921–926.
33. Matzke, R., Jacobson, K., and Radmacher, M. (2001) Direct, high-resolution measurement of furrow stiffening during division of adherent cells. *Nat. Cell Biol.* **3,** 607–610.
34. Radmacher, M., Fritz, M., Kacher, C. M., Cleveland, J. P., and Hansma, P. K. (1996) Measuring the viscoelastic properties of human platelets with the atomic force microscope. *Biophys. J.* **70,** 556–567.
35. Radmacher, M., Fritz, M., and Hansma, P. K. (1995) Imaging soft samples with the atomic force microscope: gelatin in water and propanol. *Biophys. J.* **69,** 264–270.

36. Domke, J. and Radmacher, M. (1998) Measuring the elastic properties of thin polymer films with the atomic force microscope. *Langmuir* **14,** 3320–3325.
37. Hertz, H. (1882) Über die Berührung fester elastischer Körper. *J. Reine Angew. Mathematik* **92,** 156–157.
38. Sneddon, I. N. (1965) The relation between load and penetration in the axisymmetric Boussinesq problem for a punch of arbitrary profile. *Int. J. Eng. Sci.* **3,** 47–57.